

## TopSPICE Simulations for Temperature Compensation of ISFET/MEMFET Micro-Sensor

<sup>1,2</sup> Sawsen AZZOUZI, <sup>1,2</sup> Jihen CHERMITI, <sup>1,2</sup> Mounir BEN ALI,  
<sup>1</sup> Chérif DRIDI, <sup>3</sup> Abdelhamid ERRACHID,  
<sup>3</sup> Nicole JAFFREZIC-RENAULT

<sup>1</sup> University of Sousse, Institut Supérieur des Sciences Appliquées et de Technologie de Sousse,  
Cité Ettaffala 4003 Sousse, Tunisie

<sup>2</sup> University of Carthage, Unité de Recherche de Physique des Semi-conducteurs et Capteurs,  
IPEST, La Marsa, 2070 Tunis, Tunisie

<sup>3</sup> Institut des Sciences Analytiques de Lyon, ISA, UMR 5280,  
Université Claude Bernard Lyon 1, France  
E-mail: mounirbenali@yahoo.com

Received: 31 December 2012 / Accepted: 10 August 2013 / Published: 26 May 2014

---

**Abstract:** In this work, an ISFET (Ion Sensitive Field Effect Transistor)/MEMFET (Membrane Field Effect Transistor) interface circuit with temperature compensation has been successfully designed and simulated. In each interface, we used the macro-model of ISFET/MEMFET based chemical sensors simulated in TopSPICE. The simulation results of the different sensing circuits of ISFET/MEMFETs for temperature compensation show that the readout configuration for ISFET/MEMFET sensors based on Wheatstone-Bridge connection is the most effective with a temperature drift  $5 \times 10^{-6}$  mV/°C. Copyright © 2014 IFSA Publishing, S. L.

**Keywords:** Chemical sensors, ISFETs/MEMFETs, Site-binding model, TopSPICE, Temperature compensation.

---

### 1. Introduction

In recent years there has been great progress in applying FET-type biosensors for highly sensitive ion detection. Among them, the most popular sensor ISFET (Ion Sensitive Field Effect Transistor), first introduced by Bergveld in 1970 [1], has a well-established position as a powerful sensing tool for ion detection because of his simple and clear operation principle based on site binding theory [2]. It is a solid-state device that combines the chemically sensitive membrane with a Metal-Oxide-Semiconductor Field Effect Transistor [3]. Membrane field-effect transistors (MEMFET) have

been obtained by directly coating the membrane solution onto the gate insulator surface of ISFET devices [4]. The ISFET/MEMFET sensors have features of robustness, rapid reaction time, simplicity in fabrication, low cost, high sensitivity, small size and can be implemented by CMOS technology. Despite these advantages, ISFETs/MEMFETs have been characterized indicating drawbacks related to thermal dependency. So to promote ISFET/MEMFET based applications, it is necessary to find a compensation method to reduce and cancel the temperature drift. Many research works [5, 6] have exploited different circuit architectures of readout circuits with the goal to obtain good

sensitivity as well as linearity. Most of those works usually play the role in translating the pH values to voltage domain presentation. In this context, there are many experimental works but up to now theoretical researches need more studies.

TopSPICE, the last version of SPICE, is an electrical simulator used worldwide as an essential computer-aid.

It was originally developed for designing and simulating electronic circuits but can be also adapted to design silicon-based chemical and bio-sensor Microsystems. The aim of this work is to study different architectures ensuring a temperature compensation using the TopSPICE simulation tool.

## 2. TopSPICE ISFET/MEMFET Macro-Model

The ISFET/MEMFET model can be derived from the analogous MOSFET TopSPICE model, by taking into account pH dependency of the threshold voltage.

The electrochemical properties of the insulator surface were combined with the physics of the MOSFET [7]. The ISFET static model is obtained by considering the threshold voltage  $V_{th(ISFET)}$  in the  $I$ - $V$  equations of the MOSFET [8]:

$$I_{ds} = \beta \left[ (V_{gs} - V_{th(ISFET)}) - \frac{V_{ds}}{2} V_{ds} (\text{linear region}) \right] \quad (1)$$

$$I_{ds} = \frac{1}{2} \beta (V_{gs} - V_{th(ISFET)})^2 (\text{saturation region}), \quad (2)$$

where  $\beta = (\mu C_{ox} W/L)$ , and  $\mu$ ,  $W$ , and  $L$  are the electron mobility, the channel width, and length, respectively.

The ISFET threshold voltage expression includes terms derived from MOSFET theory as well as terms related electrochemical phenomena:

$$\begin{aligned} V_{th(ISFET)} &= (E_{ref} + \phi_{lj}) - (\psi_0 - \chi_e) - \\ &- \left[ \frac{Q_{ss} + Q_{sc}}{C_{ox}} - 2\phi_f + \frac{\phi_{sc}}{q} \right] = \\ &= V_{th(MOSFET)} + E_{ref} + \phi_{lj} + \chi_e - \psi_0 - \frac{\phi_m}{q}, \end{aligned} \quad (3)$$

where  $\phi$  is the Fermi potential of the semiconductor,  $Q_{ss}$  is the fixed surface-state charge density per unit area at the insulator–semiconductor interface,  $Q_{sc}$  is the semiconductor surface depletion region charge density per unit area,  $\phi_{lj}$  is the liquid-junction potential difference between the reference solution and the electrolyte,  $\psi_0$  is the potential of the electrolyte–insulator interface that determines the ISFET sensitivity to  $H^+$  concentration,  $\chi_e$  is the electrolyte–insulator surface dipole potential,  $\phi_{sc}$  is the semiconductor work function, and  $\phi_m$  is the work function of the metal gate (reference electrode)

relative to vacuum,  $E_{ref}$  models the reference electrode according to the relationship [8]:

$$E_{ref} = E_{abs} + E_{rel}, \quad (4)$$

In equation (4),  $E_{abs}$  is the absolute potential of the standard hydrogen electrode;  $E_{rel}$  the potential of the reference electrode (Ag/AgCl considered here) relative to the hydrogen electrode.

Those terms are practically constant with respect to pH, except the potential  $\psi_0$  that depends on the pH parameter and can be calculated from the solution of the “EIS system”. Fig. 1 shows both the ISFET/MEMFET structure and the equivalent circuit corresponding; the outer connections R, D, S, B, stand for the reference electrode, the drain, the source, and the bulk, respectively.

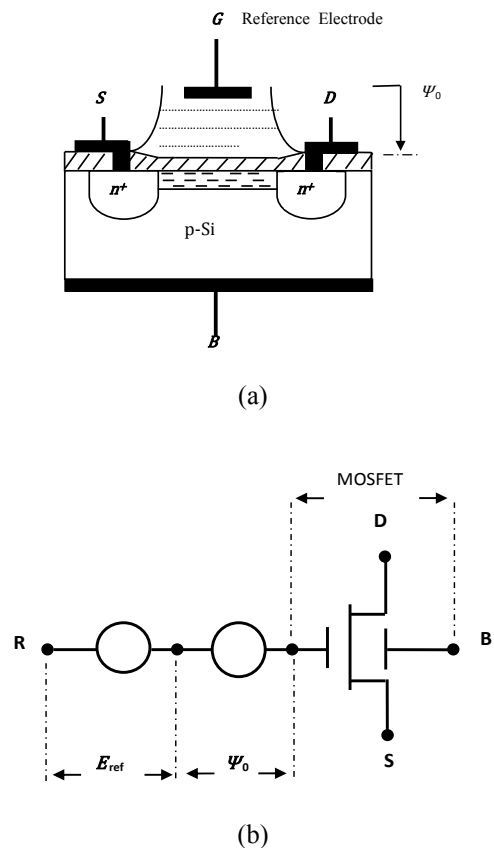


**Fig. 1.** (a) n-channel ISFET/MEMFET structure (b) Equivalent circuit of the ISFET/MEMFET.

The TopSPICE ISFET/MEMFET macro-model shown in Fig. 1(b) considers the ISFET/MEMFET sensor as two uncoupled stages: an electronic stage (The MOSFET which is the starting structure of the ISFET) and an electrochemical stage (The electrolyte–insulator interface modeled by the theory of the site-binding [9]). This macro-model was implemented in TopSPICE. It can be presented as follows in Fig. 2.

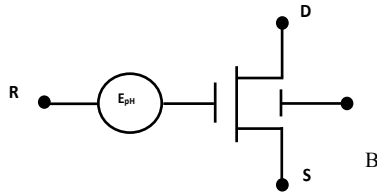


**Fig. 2.** The ISFET/MEMFET TopSPICE Macro-model.

The ISFET/MEMFET sensor is the classical MOSFET structure associated to the potential  $E_{pH}$  which depends on the reference potential  $E_{ref}$  and value as equation (5).

$$E_{pH} = -E_{ref} + \psi_0 \quad (5)$$

$$\psi_0 = 2.03 \left( \frac{\beta}{\beta + 1} \right) \left( \frac{k_B T}{qZ} \right) (pH_{pzo} - pH), \quad (6)$$

where  $\beta$  is the dimensionless pH sensitivity parameter, given by [10]:

$$\beta = \frac{2q^2 N_s}{C_s k_B T} \left( \frac{K_b}{K_a} \right)^2, \quad (7)$$

where  $C_s$  is the linearized double-layer capacitance at the insulator electrolyte interface,  $N_s$  is the surface site density,  $k_B$  is the Boltzmann's constant,  $T$  is the absolute temperature,  $q$  is the electronic charge,  $Z$  is the valence number,  $K_a$  is the acidic equilibrium constant;  $K_b$  is the basic equilibrium constant.  $pH_{pzc}$  is the pH at the point of zero charge:

$$pH_{pzc} = -1/2(pK_a + pK_b) \quad (8)$$

The proposed TopSPICE model of ISFET/MEMFET sensor is inspired from the Spice model studied in reference [11].

### 3. TopSPICE Simulation of Individual Mode

The ISFET/MEMFET operation can be obtained from both the pH-dependant characteristic and the MOSFET behavior [14]. The ISFET/MEMFET behavior has so many thermal dependencies that it is important to find a compensation method to prevent them.

In the first step, we studied the individual sensing circuit shown in Fig. 3. This circuit maintains constant drain–source voltage  $V_{ds}$  and drain current  $I_{ds}$ . The simulations were performed at  $V_{ds} = 0.8$  V and  $I_{ds} = 0.7$  mA. This contributes to the ISFET/MEMFET output characteristic's linear range. The studied dual dielectric  $SiO_2-Si_3N_4$  ISFET/MEMFET has a channel length  $L=30 \mu m$  and channel width  $W=800 \mu m$ . The simulated individual

sensing circuit is shown in Fig. 4 (a). We presented the output voltage  $V_{out}$  as function as the pH variation in Fig. 4 (b). The simulation results showed that the extracted signal  $V_{out}$  is directly proportional to the variations of pH values. In the operating pH range 1-14, the MEMFET presents a sensitivity of about 56 mV/decade.

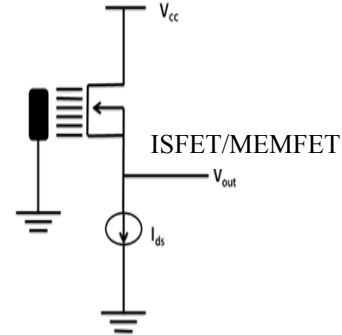


**Fig. 3.** Individual sensing circuit.

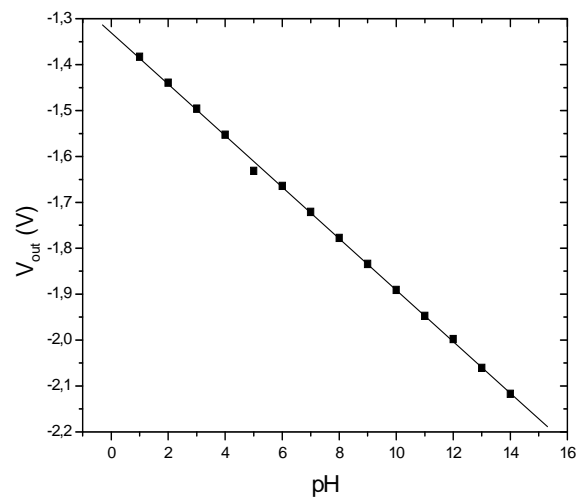
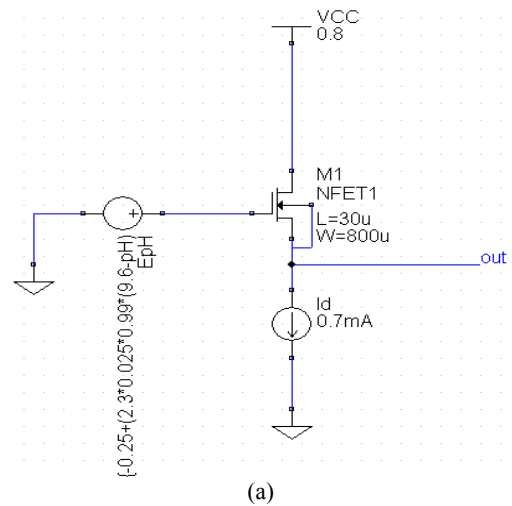


**Fig. 4.** (a) Individual simulated sensing circuit in TopSpice (b) Variation of  $V_{out}$  versus pH variation.

The temperature's effect on the output voltage  $V_{out}$  is presented in Fig. 5. We can notice that  $V_{out}$  decreases by 1 mV, when the temperature rises by 1 °C. Hence, the coefficient of temperature drift is about -1 mV / °C.

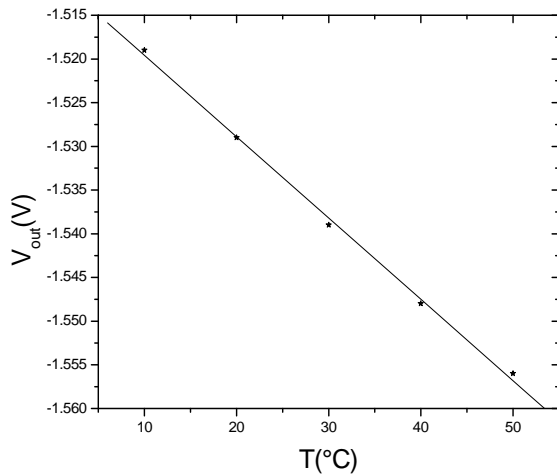


Fig. 5. Variation of  $V_{out}$  versus the temperature variation.

#### 4. TopSPICE Simulation of Differential Mode

Various studies have turned to the use and the development of differential circuits in order to improve the ISFET/MEMFET sensitivity and reduce the undesirable effects. Differential measurement is a method using an ISFET/MEMFET sensor sensitive to the detected species and a reference Field Effect Transistor. Such a reference FET (ReFET) should in ideal case show insensitivity to all species present in the sample solution [13].

##### 4.1. Sensing Circuit 1

The direct feedback configuration presented in Fig. 6 consists of a complementary pair of MOSFET and ISFET/MEMFET sensor fabricated with the same technology which can provide certain immunity on the temperature sensitivity of MOS structure of ISFET/MEMFET [14].

The two operational amplifiers fulfil a double function: (1) preserving a constant  $V_{ds}$  bias in ISFET/MEMFET and MOSFET; (2) applying the feedback signal to the reference electrode. In direct feedback configuration the drain current of ISFET/MEMFET remains constant.

$$V_{ds} = V_- = \frac{R_4}{R_3 + R_4} V_2 = \text{constant}1 \quad (9)$$

$$I_{ds} = \frac{R_4}{R_2(R_3 + R_4)} V_2 = \frac{V_{ds}}{R_2} = \text{constant}2 \quad (10)$$

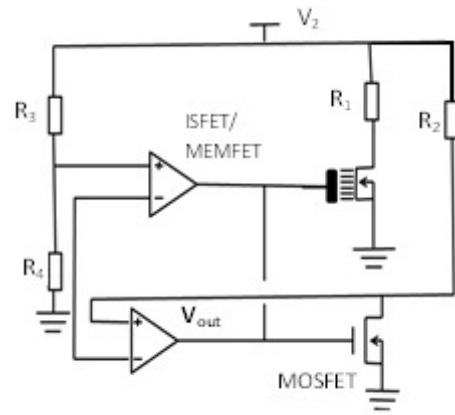
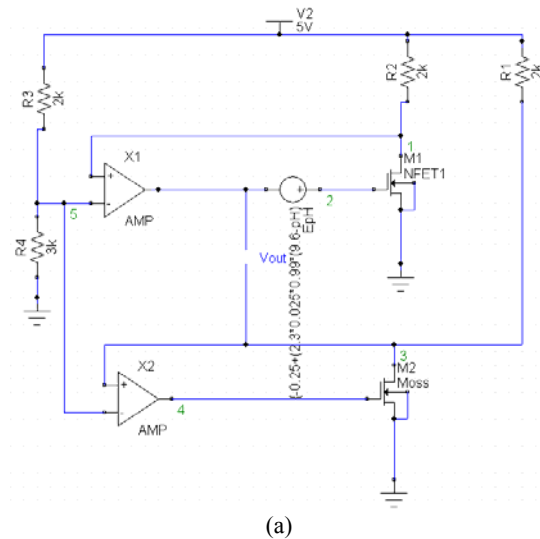
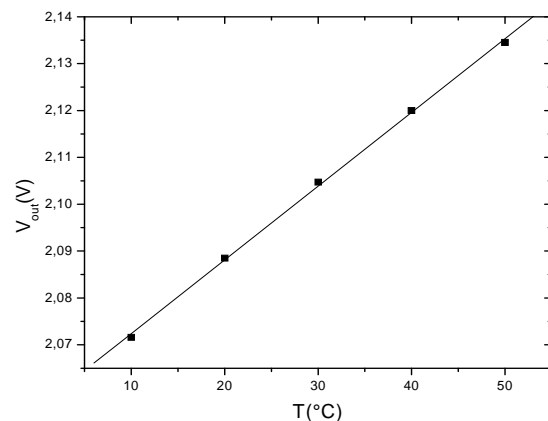


Fig. 6. Sensing circuit 1 based on a pair of ISFET/MEMFET and ReFET.

Fig. 7 (a) illustrates the simulated sensing circuit 1 in TopSPICE. The different resistance values are selected so as to optimize the sensor's sensitivity. The linear variation of the output voltage as function of the temperature showed that the thermal drift is about 1.7 mV/°C.



(a)



(b)

Fig. 7. (a) Simulated sensing circuit 1 in TopSPICE. (b) Variation of the extracted signal  $V_{out}$  versus the temperature.

### 4.2. Sensing Circuit 2

Fig. 8 illustrates the sensing circuit 2 based on a pair of ISFET/MEMFET and ReFET showing an indirect feedback configuration. The reference electrode is constantly biased. The transistor  $M_7$  (similar to transistors  $M_8$  and  $M_9$ ) controls the gate voltage of the transistor ReFET [15].

The condition  $I_2 = I_1 / 2$  must be considered to equalize the drain-source voltages of ISFET/MEMFET and ReFET. The output voltage  $V_{out}$  will follow the variations of the solution's electrochemical potential. The simulation results are shown in Fig. 9.

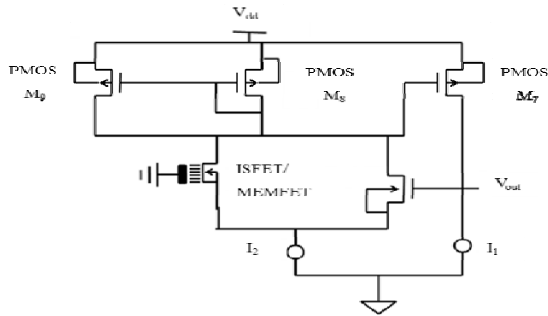


Fig. 8. Sensing circuit 2 based on a pair of ISFET/MEMFET and ReFET.

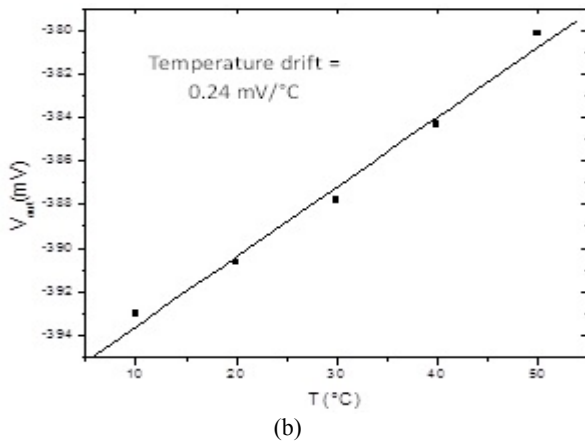
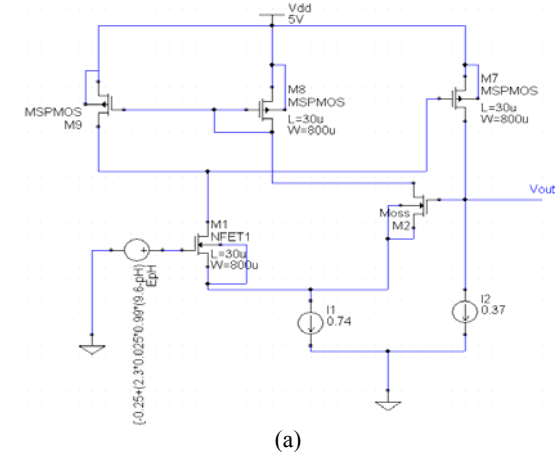


Fig. 9. (a) simulated sensing circuit 2 in TopSPICE  
(b) Variation of the output voltage  $V_{out}$  versus the temperature variation.

### 4.3. Sensing Circuit 3

The sensing circuit 3 is shown in Fig. 10. This bridge-type configuration contains a Zener diode biased bridge-type sensing circuit with the reference electrode grounded [16].

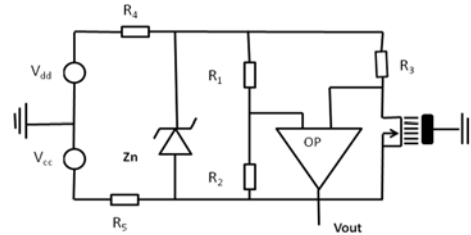


Fig. 10. Zener-based bridge-type sensing circuit.

The advantage of this configuration is grounding the reference electrode that the only one reference electrode is necessary for multiple ISFET detection. The circuit is suitable for ISFETs with unspecified characteristics because it has a wide range of operations. However, both sides of the Zener diode are floating but cannot be integrated with ISFET-based microsystem in a standard CMOS technology [17]. The simulated sensing circuit 3 in TopSPICE is shown in Fig. 11(a).

The simulation results present a linear function of a slope of unity. The temperature drift obtained from Fig. 11 (b) is 1.57 mV/°C.

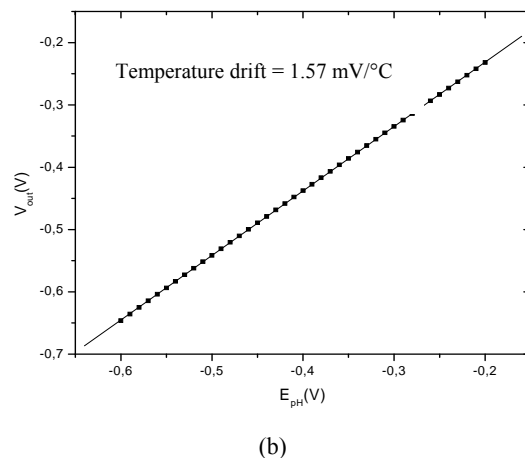
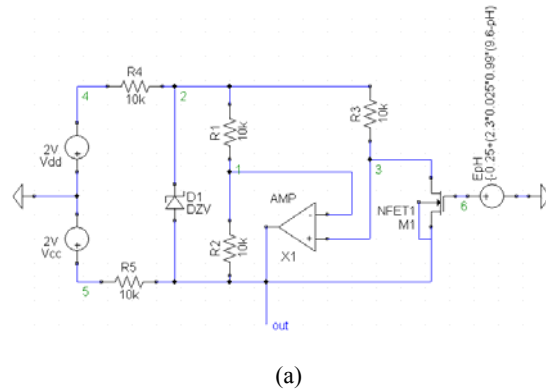


Fig. 11. (a) Simulated sensing circuit in TopSPICE  
(b) Variation of the extracted signal  $V_{out}$  as function as the temperature variation.

### 4.4 Sensing Circuit 4

The sensing circuit 4 proposed by Arkadiy Morgenshtein in 2004 [18] is capable of operating in differential mode, while allowing on chip integrations, temperature compensation, and measurements from MEMFET/ReFET pairs.

The Wheatstone-Bridge interface benefits from enhanced operational flexibility, due to the ability of relative sensitivity control of the output signal. The Fig. 12 shows the structure of Wheatstone-Bridge readout interface. An ISFET/MEMFET sensor and three MOSFET devices are applied in place of standard resistors. In order to maintain a balanced bridge, the diagonal is connected to the operational amplifier with feedback to the gate of a corresponding MOSFET. The simulated sensing circuit 4 in TopSPICE is presented in Fig. 13.

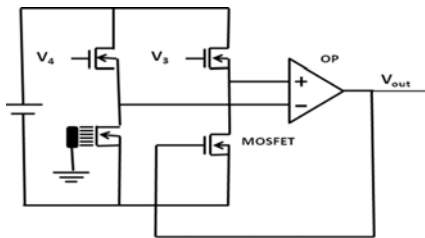


Fig. 12. Wheatstone bridge of readout interface.

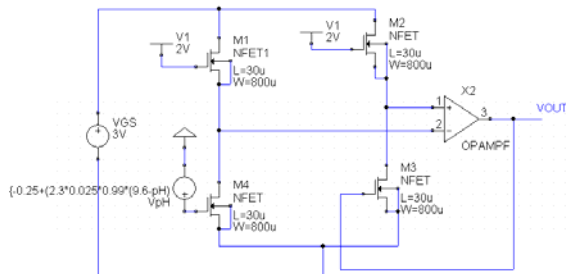


Fig. 13. Simulated sensing circuit 4 in TopSPICE.

Fig. 14 shows a linear variation of the output voltage versus the temperature. Then, we note that the coefficient of the temperature drift is about

$5 \times 10^{-6} \text{ mV} / ^\circ\text{C}$ . This result demonstrates a very good compensation of the temperature influence.

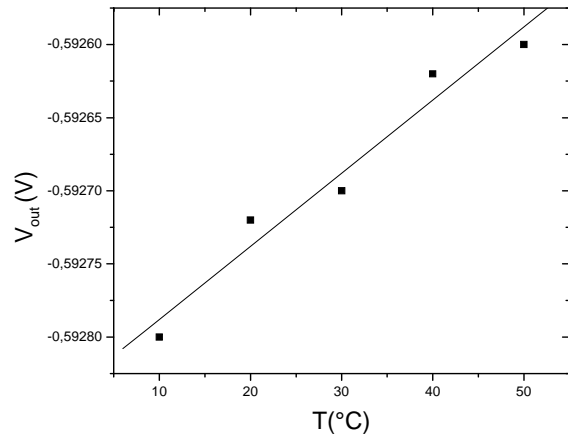


Fig. 14. Temperature's variation of the extracted signal  $V_{out}$ .

### 4.5. Comparative Studies of Performances of Different Sensing Circuits

The study of the various sensing circuits (individual and differential mode) shows that the output voltage is directly proportional to the pH values variation. This reflects the linearity of the overall system (sensor + conditioner) which is an advantage for all studied circuits.

The Table 1 summarizes the different ISFETs/MEMFETs sensitivities. One can observe that for a given valency number Z, the sensitivity remains practically constant (56.6 mV/decade for Z=1) for the different sensing circuits. Hence, signal conditioning does not affect the sensor's sensitivity.

Also, for a given sensing circuit, it has been demonstrated that the ISFET/MEMFET simulated sensitivities for the different valence numbers Z (1 to 4) are in good agreement with the nernstian sensitivities of the MEMFET sensor [19, 20] based on the site binding theory.

Table 1. Different ISFET/MEMFETs sensitivities for different valence number Z (1 4).

Valence number Z)	Sensitivity (mV/decade)				Theoretical MEMFET sensitivity (mV/decade)
	Sensing circuit 1	Sensing circuit 2	Sensing circuit 3	Sensing circuit 4	
1	56.6	56.8	56.9	56.1	59.0
2	28.3	28.4	28.4	28.0	29.5
3	18.8	18.9	18.9	18.7	19.6
4	14.2	14.2	14.2	14.0	14.7

Table 2 shows that the Wheatstone bridge circuit can ensure the better temperature compensation ( $5 \times 10^{-6}$  mV/°C).

**Table 2.** Different thermal drifts for the various ISFET/MEMFET sensing circuits.

Sensing circuit	Sensing circuit 1	Sensing circuit 2	Sensing circuit 3	Sensing circuit 4
Temperature Drift (mV/°C)	1.7	0.24	1.57	$5 \times 10^{-6}$

## 5. Conclusions

The presented instrumentation with various electronics circuits has been developed to compensate the thermal dependence of ISFET/MEMFET based chemical micro-sensors. To check the validation of the proposed circuits, TopSPICE simulation of functionality for sensitivity was performed. A TopSPICE macro-model considered the ISFET/MEMFET as two stages (an electronic stage and an electrochemical stage) has been developed. In the first step, the simulation results show that the extracted signal  $V_{out}$  voltage is directly proportional to the variations of pH values ( $S_T=56.6$  mV/decade). Then, using the same methodology, we extrapolate our simulation to the MEMFET devices and we noted that the sensitivity remains practically constant for a given valence number  $Z$ . We have also demonstrated that, for a given sensing circuit, the ISFETs/MEMFETs simulated sensitivities for different valence number  $Z$  (1 to 4) are in good agreement with the theoretical MEMFET sensitivities. In addition, it was shown in particular that the Wheatstone bridge circuit ensures the better temperature compensation. Hence, the proposed temperature sensitivity compensation method based on Wheatstone-Bridge circuit not only gives a more accurate pH measurement, but also improves the thermal stability of the ISFET/MEMFET for the increasing chemical sensors applications.

## Acknowledgements

This work was partially supported by the NATO Science for Peace (SFP) Project CBP. NUKR. SFP 984173.

## References

- [1]. P. G. Fernandes, H. J. Stiegler, M. Zhao, K. D. Cantley, B. Obradovic, R. A. Chapman, H. C. Wenc, G. Mahmud, E. M. Vogel, SPICE macromodel of silicon-on-insulator-field-effect-transistor-based biological sensors, *Sensors and Actuators B*, Vol. 161, 2012, pp. 163–170.
- [2]. P. Bergveld, Thirty years of ISFETOLOGY what happened in the past 30 years and what may happen in the next 30 years, *Sensors and Actuators B*, Vol. 88, 2003, pp. 1–20.
- [3]. W. Y. Chung, F. S. He, C. H. Yang, M. C. Wang, Drift Response Macromodel and Readout Circuit Development for ISFET and its  $H^+$  Sensing Applications, *Journal of Medical and Biological Engineering*, Vol. 26, Issue 1, 2005, pp. 29-34.
- [4]. A. Errachid, C. P. Jiménez, J. Casabo, L. Escriche, J. A. Munoz, A. Bratov, J. Bausells, Perchlorate-selective MEMFETs and ISEs based on a new phosphadithiamacrocycle, *Sensors and Actuators B*, Vol. 43, 1997, pp. 206–210.
- [5]. P. K. Chan, D. Y. Chen, A CMOS ISFET Interface Circuit With Dynamic Current Temperature Compensation Technique, *IEEE Transactions on Circuits and Systems*, Vol. 54, 2007, pp. 119-128.
- [6]. D. Y. Chen, P. K. Chan, M. S. Tse, A CMOS ISFET interface circuit for water quality monitoring, *IEEE Conf. Sensors*, Irvine, CA pp. 1217–1220, 2005.
- [7]. P. D. Batista, M. Mulato, C. F. de O. Graeff, F. J. Fernandez, F. das C. Marques, SnO<sub>2</sub> extended gate Field-effect transistor as pH sensor, *Brazilian Journal of Physics*, Vol. 36, Issue 2A, 2006.
- [8]. S. Martinoia, G. Massobrio, L. Lorenzelli, Modeling ISFET microsensor and ISFET-based microsystems: a review, *Sensors and Actuators B*, Vol. 105, 2005, pp. 14–27.
- [9]. S. Martinoia, P. Massobrio, ISFET–neuron junction: circuit models and extracellular signal simulations, *Biosensors and Bioelectronics*, Vol. 19, 2004, pp. 1487–1496.
- [10]. J.-C. Chou, L. P. Liao, Study on pH at the point of zero charge of TiO<sub>2</sub> pH ion-sensitive field effect transistor made by the sputtering method, *Thin Solid Films*, Vol. 476, 2005, pp. 157 – 16.
- [11]. M. Daniel, M. Janicki, A. Napieralski, Simulation of Ion Sensitive Transistors Using a SPICE Compatible Model, in Proceedings of the *IEEE International Conference on Sensors (IEEE Sensors)*, 2003, pp. 596–597.
- [12]. W. Y. Chung, C. H. Yang, D. G. Pijanowska, P. B. Grabiec, W. Torbic, ISFET performance enhancement by using the improved circuit techniques, *Sensors and Actuators B*, Vol. 113, 2006, pp. 555–562.
- [13]. M. S. Ptasińska, P. D. Van Der Wal, A. Van Den Berg, P. Bergveld, E. J. R. Sudholter, D. N. Reinhoudt, Reference field effect transistor based on chemically modified ISFETs, *Analytica Chimica Acta*, Vol. 230, 1990, pp. 67-73.
- [14]. A. Sibbald, A chemical-sensitive integrated-circuit: The operational transducer, *Sensors and Actuators*, Vol. 7, 2006, pp. 23–38.
- [15]. I. Humenyuk, Développement des microcapteurs ChemFETs pour l'analyse de l'eau, Ph. D. Thesis, *Institut National des Sciences Appliquées de Toulouse*, 2005.
- [16]. W. Y. Chung, Y. T. Lin, D. G. Pijanowska, C. H. Yang, M. C. Wang, A. Krzyskow, W. Torbic, New ISFET interface circuit design with temperature compensation, *Microelectronics Journal*, Vol. 37, 2006, pp. 1105–1114.
- [17]. W. Y. Chung et al, US Patent N. 6 906 524 B2, June 2005.

- [18]. A. Morgenshtein, L. S. Boreysha, U. Dinnar, C. G. Jakobson, Y. Nemirovsky, Wheatstone-Bridge readout interface for ISFET/REFET applications, *Sensors and Actuators B*, Vol. 98, 2004, pp. 18–2.
- [19]. R. Kalfat, M. Ben. Ali, R. Mlika, F. F. Romdhane, N. J. Renault, Polysiloxane–gel matrices for ion sensitive membrane, *International Journal of Inorganic Materials*, Vol. 2, 2000, pp. 225–231.
- [20]. M. Ben Ali, R. Mlika, H. B. Ouada, R. M'ghaieth, H. Maaref, Porous silicon as substrate for ion sensors, *Sensors and Actuators*, Vol. 74, 1999, pp. 123–125.

2014 Copyright ©, International Frequency Sensor Association (IFSA) Publishing, S. L. All rights reserved.  
(<http://www.sensorsportal.com>)

## Universal Sensors and Transducers Interface (USTI)

for any sensors and transducers with frequency, period, duty-cycle, time interval, PWM, phase-shift, pulse number output



The image shows three USTI chips: a small square chip, a medium square chip, and a large DIP package. To the left of the chips are five white icons on a dark red background: a square wave, a variable capacitor, a variable resistor, a Wheatstone bridge, and a gear.

- \* Input frequency range: 0.05 Hz ... 9 MHz (144 MHz)
- \* Selectable and constant relative error: 1 ... 0.0005 % for all frequency range
- \* Scalable resolution
- \* Non-redundant conversion time
- \* RS232, SPI, I2C interfaces
- \* Rotational speed, *rpm*
- \* Cx, 50 pF to 100  $\mu$ F
- \* Rx, 10  $\Omega$  to 10 M $\Omega$
- \* Pt100, Pt1000, Pt5000, Cu, Ni
- \* Resistive Bridges
- \* PDIP, TQFP, MLF packages

**Just make it easy !**

<http://www.techassist2010.com/>    [info@techassist2010.com](mailto:info@techassist2010.com)